Politecnico di Milano

Department of Aerospace Sciences and Technologies

AY 2018-2019

Professor: *Camilla Colombo*

Orbital Mechanics

Interplanetary Explorer Mission – Planetary Explorer Mission

Group 39

Authors:

Cod. persona	Name	Last Name
10503063	Andrea	Bacchiega
10662446	Chrystle	Dzousa
10482528	Gianluca	Lardo
10494079	Davide	Viviani

TABLE OF CONTENTS

1.Symbols

Area	A	$[m^2]$
Argument of periapsis	ω	*[deg]*
Earth's angular rate	ω_E	*[rad/s]*
Eccentricity	e	*[-]*
Frequency	f	*[Hz]*
Gravitational parameter	μ	$[km^3/s^2]$
Heliocentric distance	R	*[km]*
Heliocentric velocity	V	*[km/s]*
Inclination	i	*[deg]*
Latitude	φ	*[deg]*
Longitude	λ	*[deg]*
Mass	m	*[kg]*
Mean anomaly	M	*[deg]*
Orbital period	T	*[s]*
Pressure	P	$[N/m^2]$
RAAN	Ω	*[deg]*
Reflectivity	C_R	*[-]*
Relative distance	r	*[km]*
Relative velocity	v	*[km/s]*
Semi-major axis	a	*[km]*
True anomaly	ϑ	*[deg]*

Data

Constants:

Gravitational acceleration	g	9,81	$\frac{m}{s^2}$
Earth's Radius	R_E	6371	*km*

Flight path for assignment 1

Uranus → Mars → Mercury

Initial parameters for assignment 2

Perturbation	*a*	*e*	*i*	Ω	*ω*	*ϑ*
SRP	8000 km	0,005	7°	40°	45°	20°

$"_E"\ subscripts\ refer\ to\ "Earth",\quad "_S"\ subscripts\ refer\ to\ "Sun"$

2.Assignment 1

Interplanetary Explorer Mission

The PoliMi space agency is carrying out a feasibility study for an *Interplanetary Explorer Mission,* visiting three different planets in the Solar System, which are Uranus, Mars and Mercury. The mission will depart from Uranus, and it will fly toward Mercury exploiting a GA flyby from Mars.
This report aims to perform a *preliminary mission analysis*, considering different strategies to find what could be the best solution for this mission. The figure of merit, upon which we will make our final choice, will primarily be the mission cost (measured through the ΔV needed to perform the manoeuvres). Moreover, another parameter, that will be crucial in the analysis, will be the total ToF, in order to complete the mission in a reasonable time.

2.1 Design Process

The mission aims to perform an interplanetary fly using the *patched-conic methods*, solving the problem with two *Lambert's Arcs.* The flight will occur from Uranus, to Mercury, with the flyby of Mars. Departure from Uranus and orbit insertion on Mercury is not taken into account in this analysis, thus assuming initial and final state vectors equal to those of the respective planets. Time of flight in the two legs of the Lambert's Arcs, as well as the amount of mission cost, will be strongly considered for the completion of the mission. For computing the solution, we perform a *grid search* throughout a 3D array.

The optimal solution will be chosen, with some consideration on feasibility and time constraints.

2.1.1 Design Constraints

The time window, for the mission to start, regards a crucial point in the mission analysis. Therefore, it is important to analyse first the possible departure times over a wide range. That should be chosen wisely, accordingly with a reasonable choice between computational costs and effective benefits on mission costs. However, the range of departure dates would not affect considerably the results, because Uranus is an outer planet and his period is about 84 years. Therefore, in a departure window of 3-4 years, it will cover a small part of his orbit . The choice of the ToF is a degree of freedom too. The satellite should be able to move to the optimized orbit, and this may be longer than expected, as it would be shown in the results. The range for the flyby and the capture in Mercury must be at least one synodic period to ensure that all the possible relative positions between Mars and Mercury have been considered.

	Mars	Mercury
Period	687 days	88 days

The synodic period of Mercury and Mars is:

$$Tsyn = \frac{T_1 T_2}{(T_1 - T_2)} = \ 100{,}92 \text{ days}$$

As said before, the maximum allowed departure date is limited, setting it before 2022. Another parameter, to take consideration of, is the height of the flyby. Of course, it is fundamental to choose an altitude high enough so that Mars's atmosphere does not interfere with the spacecraft trajectory.

2.1.2 Grid Search Setup

Using a *triple loop 'for' cycle*, it is possible to obtain a matrix with many different departure times and arrival times, including the three coordinates for velocity. In this way, with the cycle it is possible to select a different departure window, comparing it with the total amount of velocity required from the mission. Of course, the cycle takes consideration only of plausible departure times, in order to fit the mission in a reasonable time.

The cycle allows us to estimate a different set of Lambert's Arcs, giving an estimation of the best suitable solution. It is useful to do a preliminary examination of a wide range of departure times, then, to refine the grid for a finer scan on the time window preferred. The algorithm is as precise as the time intervals are smaller, but this increases considerably the amount of time needed to perform the computation. Hence, it is not reasonable to look for the absolute minimum (in terms of ToF and mission cost), but to choose the best trade-off for the mission. It has been decided to take a time span 25 days for a first approach.

The algorithm considers every possible combination of departure, flyby and arrival. For every flyby date it is calculated every combination of departure and arrival, and then the results are compared to find the optimal solution. If the overall cost is lower than the previous one, and does exist a feasible flyby, the result is saved.

The result will be a matrix of dimension [departure dates x arrival dates] where every element contains the information about the best flyby solution.

2.1.3 Selection of a Final Solution

The lowest cost is achieved in correspondence of:

Departure	*Flyby*	*Arrival*	*ΔV [km/s]*
16 nov 2022	11 nov 2044	26 dec 2051	30.5626

which is nevertheless unacceptable, due to the excessive transfer time (almost 30 years).

We set instead the optimization of the cost and a limitation on the time of flight of 15 years. This yields as optimum:

Departure	*Flyby*	*Arrival*	*ΔV [km/s]*
01 Jan 2020	18 Aug 2033	20 May 2035	46.4876

which the team has eventually selected as the final compromise-solution.

In order to corroborate the validity of our design choices, the porkchop plot might be selected as a first validation tool. It can be experienced that the burn in correspondence of the PGA tends to be significant in magnitude, even in the case of high time of flight. If we plot porkchop diagrams, separately considering each arc just as if they were uncoupled problems (temporarily neglecting the value of the burn performed at the flyby planet), we will see that our optimal solution does not lie in an optimal zone for Uranus-Mars transfer.

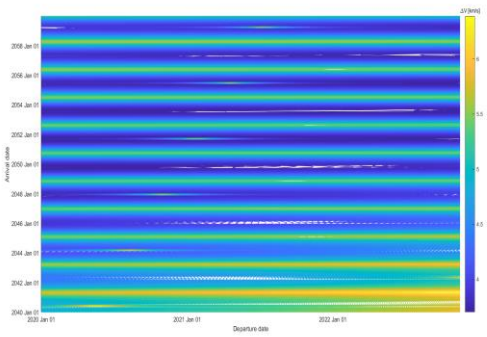

Figure 1.1 Porkchop plot for Uranus→Mars transfer

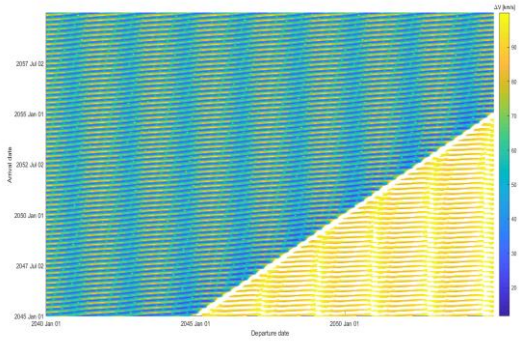

Porkchop plot for Mars→Mercury transfer

2.2 Results and Conclusions

2.2.1 Heliocentric Trajectories

We hereby show here the outcomes of the final solution for the two heliocentric trajectories (Lambert's Arcs) as keplerian parameters:

	Departure	*Arrival*	*a [km]*	*e*	*i*	*Ω*	*ω*	$\boldsymbol{\theta_{dep}, \theta_{arr}}$
Uranus → Mars	*01 Jan 2020*	*18 Aug 2033*	*8.829*10^8*	*0.998*	*0.033*	*2.46*	*0.35*	*3.28, 8.83*
Mars →Mercury	*18 Aug 2033*	*20 May 2035*	*2.320*10^8*	*0.765*	*0.032*	*2.17*	*0.83*	*2.35, 7.27*

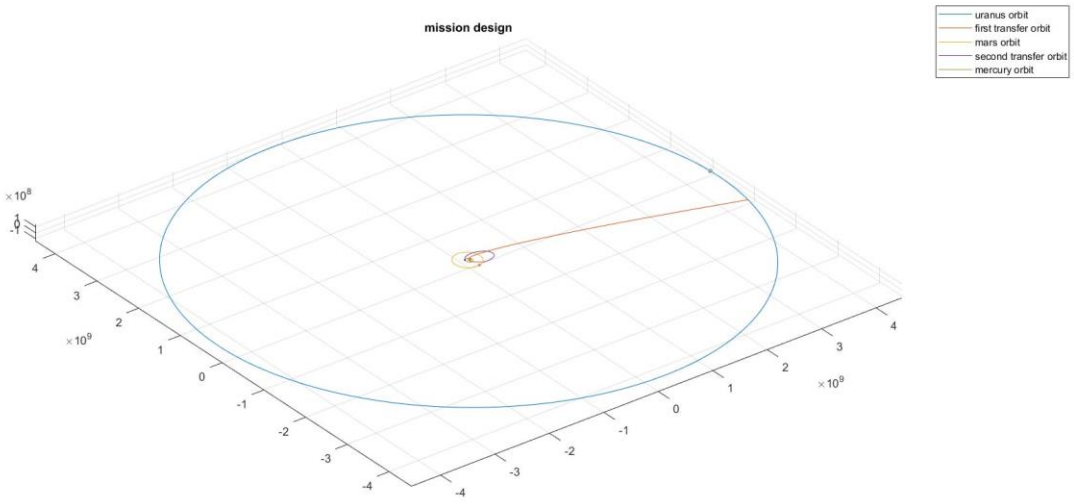

Figure 1.2 Mission Design

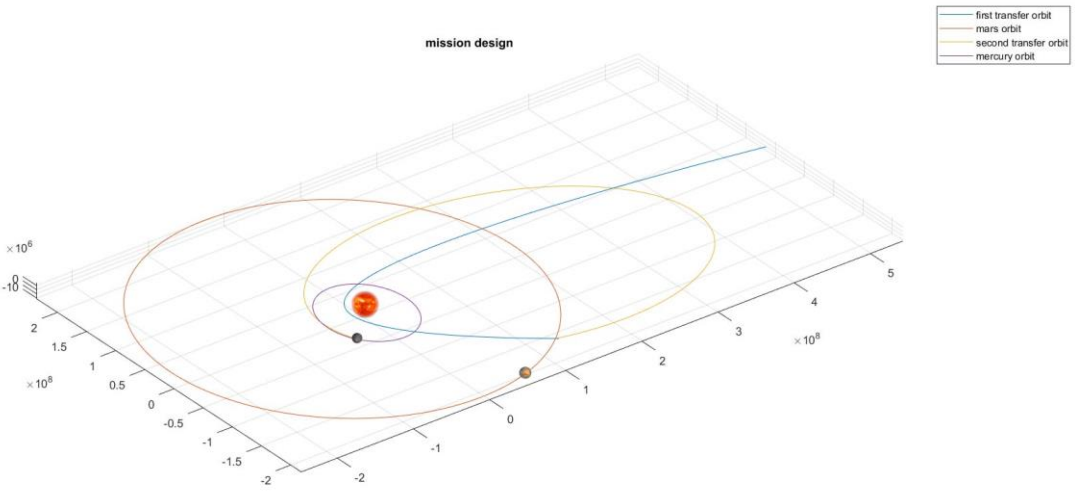

Figure 1.3 Mission Design [detailed]

2.2.2 Powered Gravity Assist

The velocities on the flyby hyperbola has been rescued from the incoming and outcoming leg of the Lambert's Arcs. Since V_∞^+ and V_∞^- will in general differ from each other, the flyby is required to be powered: an impulsive burn $\Delta V_{PGA} = 15.12\ km/s$ is enhanced at the perigee of the two hyperbolic arcs. Hereby we show the results obtained after the computation:

$\Delta V = \|V^+ - V^-\|$	$V_\infty^-\ km/s$	$V_\infty^+ km/s$	e-	e+	$r_p\ km$
15,12	*38,36*	*22,49*	*149,7*	*52,88*	*4385*

Where V_∞^- and V_∞^+ results are:

V_∞^- = [28.83; -20.57; -0.96] km/s **V_∞^+ = [25.81; -5.60; -0.73] km/s**

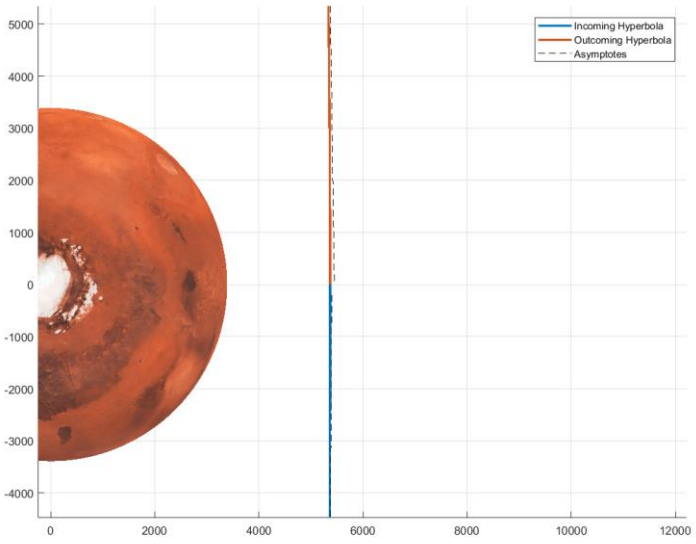

Figure 1.4 Flyby

2.2.3 Mission Cost Analysis

The mission cost, is displayed in the table below, as values of *ΔV,* respectfully for departure, flyby, arrival, and the total amount. All values are expressed in km/s. The following table shows the results:

Departure	*Flyby*	*Arrival*	*ΔV*
8.28	15.12	23.11	46.48

Besides these results supposedly being the best trade-off in terms of propellant cost and time of flight, they probably would not be feasible for a real-life mission: the overall ΔV is still too high for a state of the art upper-stage to achieve. During the analysis, two main possible solutions to the problem have been identified:

- Increase the total ToF. Whenever the overall time of the mission is increased, the total optimal cost of the mission drops asymptotically to a magnitude around 30 km/s. This, indeed, would be a value that the state of the art engines could not reach. The very high duration of the mission (30 years) makes it further unsuitable for any scientifically significant mission.

- Increase the number of Flybys. For this mission analysis, it was required to perform only one gravity assists during the cruise from Uranus to Mercury. In a real-life mission, a larger number of gravity assists could be performed in order to exploit their ability to increase the heliocentric speed of the spacecraft. This would reduce the overall cost of the mission, making the transfer between the two planets at least plausible with the current technologies. This consideration is indeed supported by actual past missions' data: Voyager II performed 3 flybys before reaching Neptune, with technologies already available over 40 years ago.

In this analysis, the close passage to the Sun, in the first transfer orbit, has not been taken into account. A further analysis, detailing the passage that is the closest to Sun, has to be done for the overall feasibility of the final solution.

3.Assignment 2

Planetary Explorer Mission

The PoliMi Space Agency wants to launch a *Planetary Explorer Mission*, to perform Earth observation. The mission aims at studying the effect of orbit perturbations. The study will be done considering the J2 effect and, in a second time, also the Solar Radiation Perturbation (SRP) will be taken into account. To do so, there will be a comparison between different implementation methods for orbit. A frequency analysis will show the main harmonics associated with the perturbing effects. A ground track estimation will be given, as well as some orbit corrections to achieve a repeating ground track. In the end, a comparison with satellite TDRS-3 is shown, as a figure to evaluate the estimation.

3.1 Initial Orbit Characterization

The orbital elements for the characterization of the initial Earth-centred orbit are the following:

a	e	i
8000 km	0,005	7°
Ω	ω	ϑ
40°	45°	20°

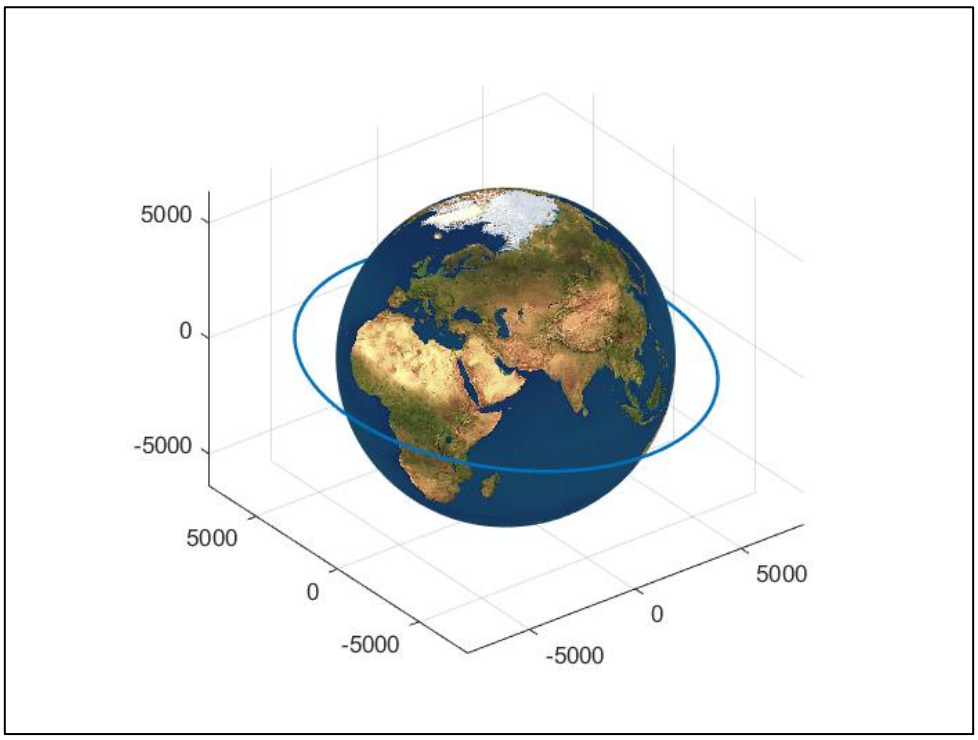

Figure 2.1 Initial orbit

The perturbations that will be considered are:

- J2 effect (Earth Oblateness):

$$\boldsymbol{a}_{J2} = \frac{3}{2}\frac{J_2 \mu {R_E}^2}{r^5}\left\{\left(5\frac{z^2}{r^2}-1\right)x\boldsymbol{i} + \left(5\frac{z^2}{r^2}-1\right)y\boldsymbol{j} + \left(5\frac{z^2}{r^2}-3\right)z\boldsymbol{k}\right\} \quad (3.1)$$

- Solar Radiation Pressure (SRP):

$$\boldsymbol{a}_{srp} = p_{sr@1AU}\left(\frac{AU}{r_{S\to S/C}}\right)^2 C_R \frac{A}{m}\boldsymbol{r}_{S\to S/C} \quad (3.2)$$

For SRP an area-to-mass ratio $\frac{A}{m} = 0{,}5\ m^2/kg$ will be assumed, along with a reflectivity $C_R=1$.

3.2 Ground Track

During the flight of a satellite on its trajectory, the ground track will be affected by a westward shift. This is due to two main effects: the *Earth rotation* and its oblateness, which causes a *J2 perturbation* with a secular effect on the RAAN. To quantify the perturbation we use:

$$\Delta\Omega_{TOT} = -\frac{2\pi T_E}{T} + \left(-\frac{3\pi J_2 {R_E}^2 \cos i}{(1-e^2)^2 a^2}\right) \quad (3.3)$$

The first term of the sum refers to the Earth's rotation, while the second one takes consideration of the J2 effect. The orbit is close to the equator, which increases the J2 effect on the orbit perturbation with respect to another orbit closer to the poles. Below, there is a comparison between the orbit propagation with, and without the J2 effect over different periods. The ground tracks were plotted for the time periods of 1 orbit revolution, 1 day and 10 days, respectively.

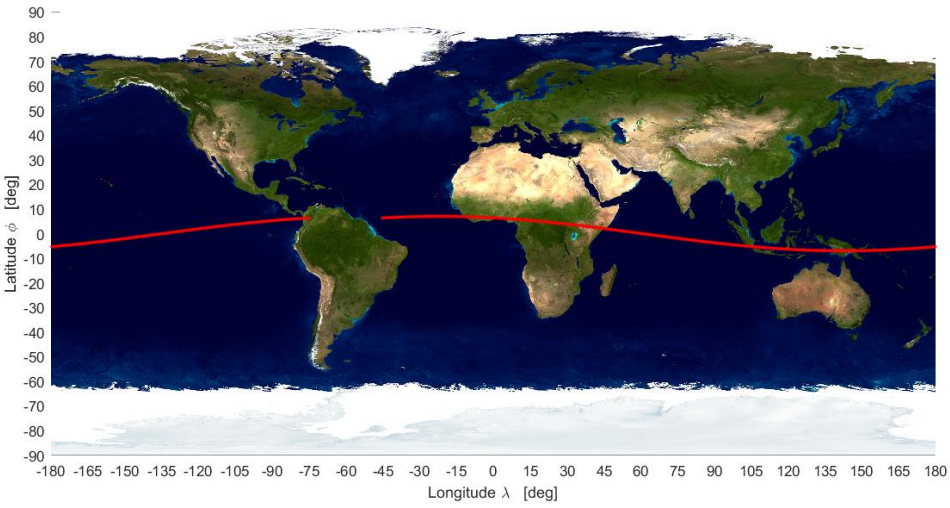

Figure 2.2 Groundtrack over 1 period

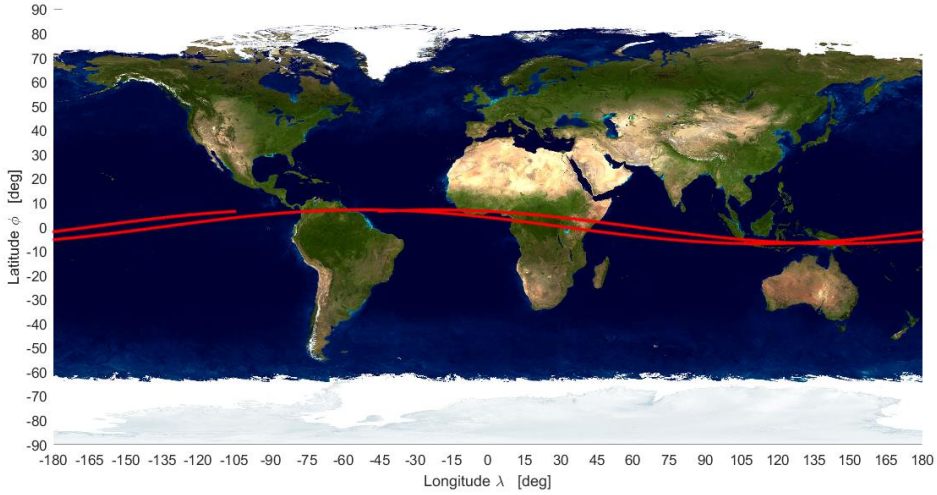

Figure 2.3 Groundtrack over 2 periods

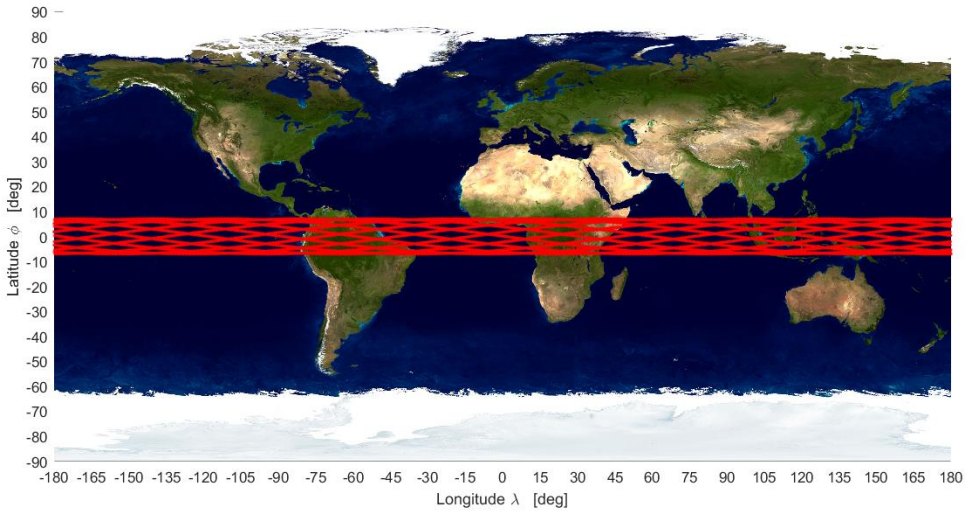

Figure 2.4 Groundtrack over 10 days

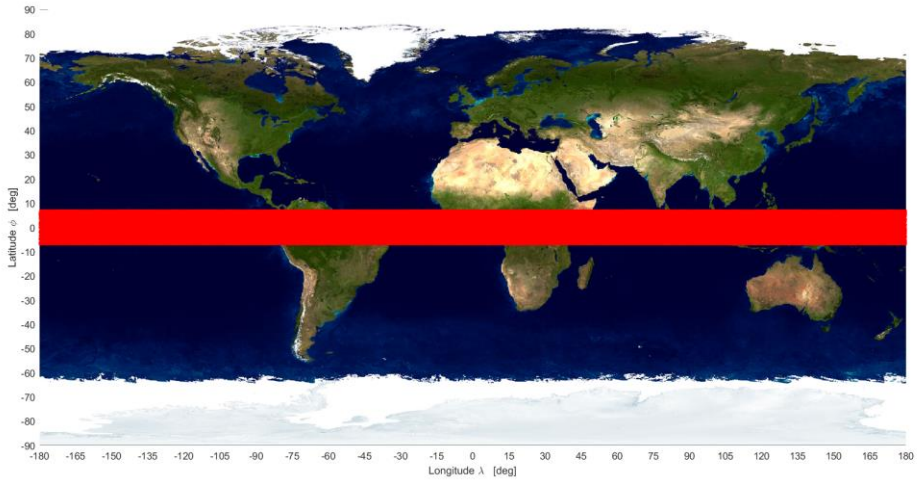

Figure 2.5 Groundtrack over a long period

3.2.1 Ground Track Repetition

To force the ground track repetition we do the following operation to the period:

$$m2\pi = n\Delta\Omega_{TOT} \quad (3.4)$$

where *n* is the number of orbital periods, and *m* is the number of sidereal days before the repetition.
In order to make the groundtrack repeating we modified the semimajor axis, adapting it to the number of orbit, after which the repetion had to occur. We choose a number of four revolutions to make the repetion happen and the semi-major axis has been modified has follow:

“ n_period = 4;

n_orb_rep = n_period;

*a_rep = ((((2*pi/(n_period*w_e))^2)*(mu/(4*(pi^2)))))^(1/3); “*

where, to make it easier to read, a_{rep} is:

$$a_{rep} = \left(\frac{2\pi}{n_{period} * \omega_E}\right)^2 * \sqrt[3]{\frac{\mu}{4\pi^2}} \quad (3.5)$$

The obtained value of semi-major axis has been taken for all the rest of the assignment, without any other modification.

For the ground track to repeat over different orbital periods, it was necessary to insert a modification. This has been identified in a little alteration of semi-major axis parameter.

	Original orbit	***Modified orbit J2 (off)***	***Modified orbit J2 (on)***
a [km]	**8000 km**	**16733**	**16733**

It is possible to notice that the modification would be quite small compared to the initial orbit. It remains precise enough for a ground track over a certain spot on the Earth’s surface. Moreover, even with a modified semi-major axis, it is not possible to obtain a ground track that repeats exactly when taking the J2 effect in consideration.

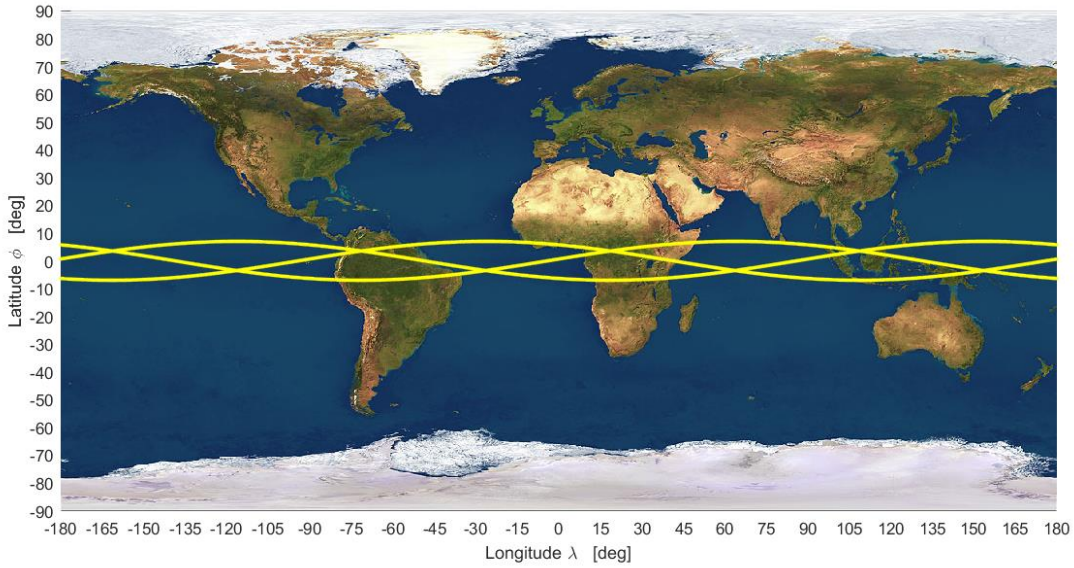

Figure 2.6 Groundtrack with J2 effect

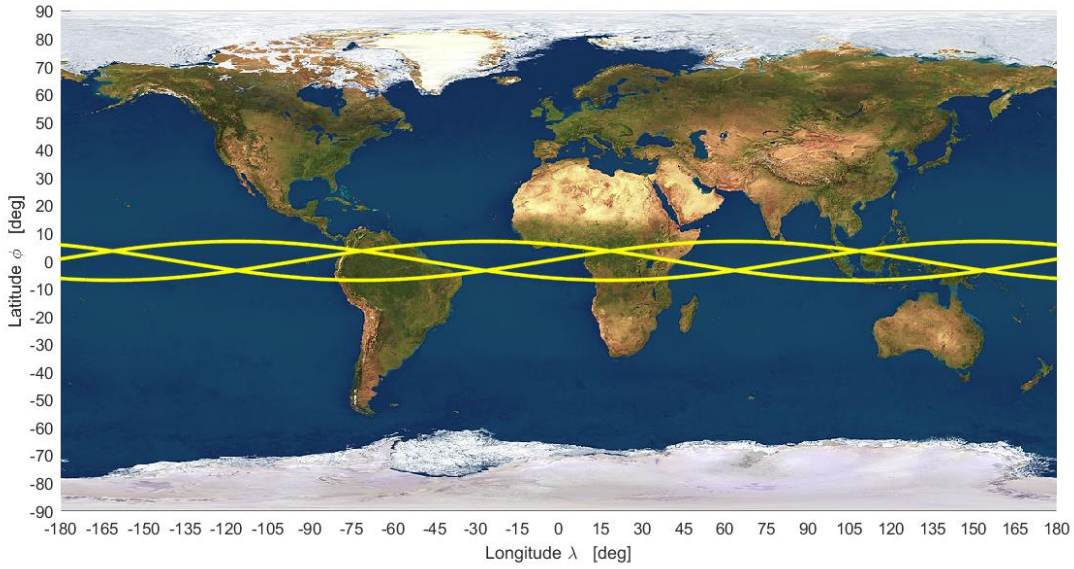

Figure 2.7 Groundtrack with J2 and SRP effect

The reason was hypothesized to be inherently associated with the nature of the perturbed two body problem.

The gravitational perturbation due to J2 determines secular effects not only in terms of nodal regression but also changes the argument of perigee and the mean anomaly.

3.3 Orbit Propagation

It is possible to propagate the orbital elements, in order to see the orbit evolution over different period of times. To do so, it is possible to choose between two different methods: one uses *Cartesian coordinates*, the other one the *Gauss planetary equations*.

Taking into account the importance of accuracy through long-term prediction of the orbit, a span of 25 years was considered from 2020/01/01 and 1 million points were used for integration. To analyse the trend, orbital elements were propagated over time using the conventional Cartesian method and the Gauss method.

The graphs are in accordance with the theory for the prograde orbit where we can observe the trend of decreasing RAAN and increasing perigee anomaly. The difference in variations is small.

A substantial difference may be highlighted in terms of computational efficiency: computation timing was estimated for Cartesian and Gauss method. It turned out that the Cartesian method took around 1.27 hrs, while the Gauss method took around 30 mins. Therefore, Gauss revealed to be less expensive and quicker, since it incorporated the direct evolution of keplerian elements. For the range of discretization, levels covered in this plot, Gauss planetary equations are about twice as quick as Cartesian coordinates integration.

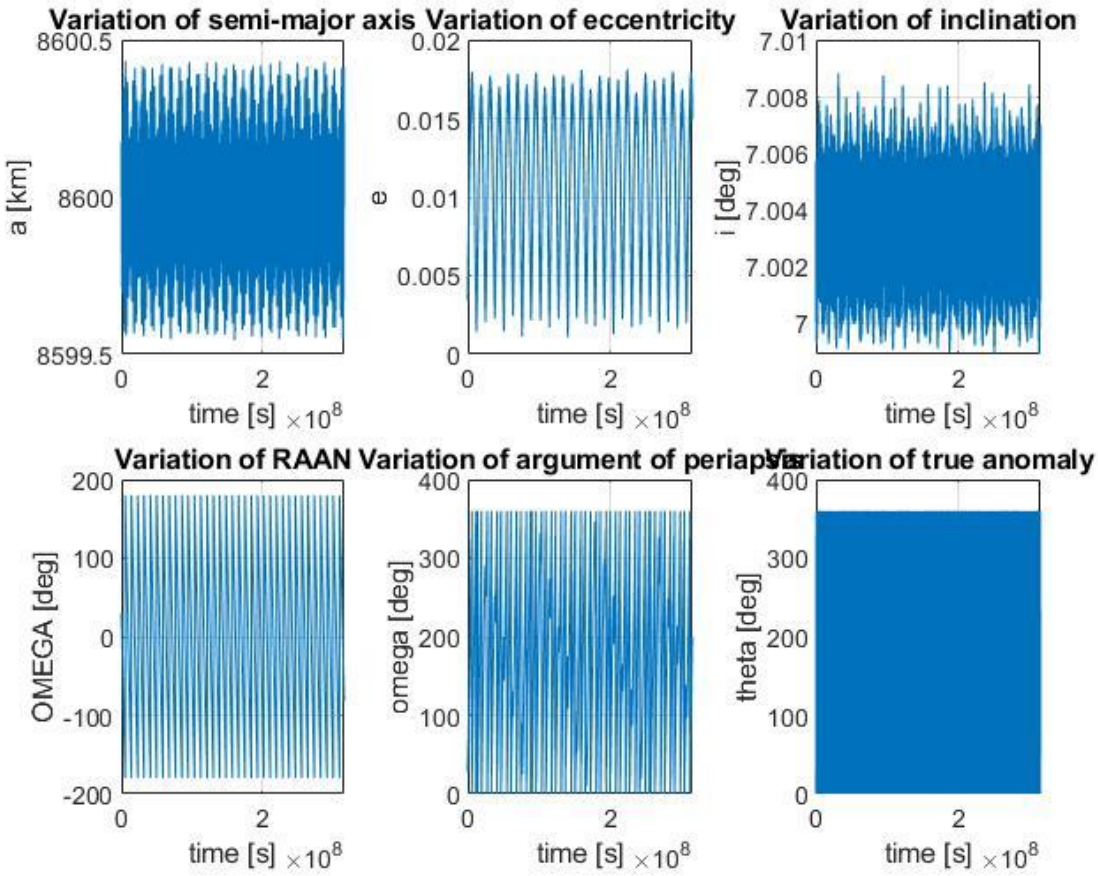

Figure 2.8 Cartesian Variation

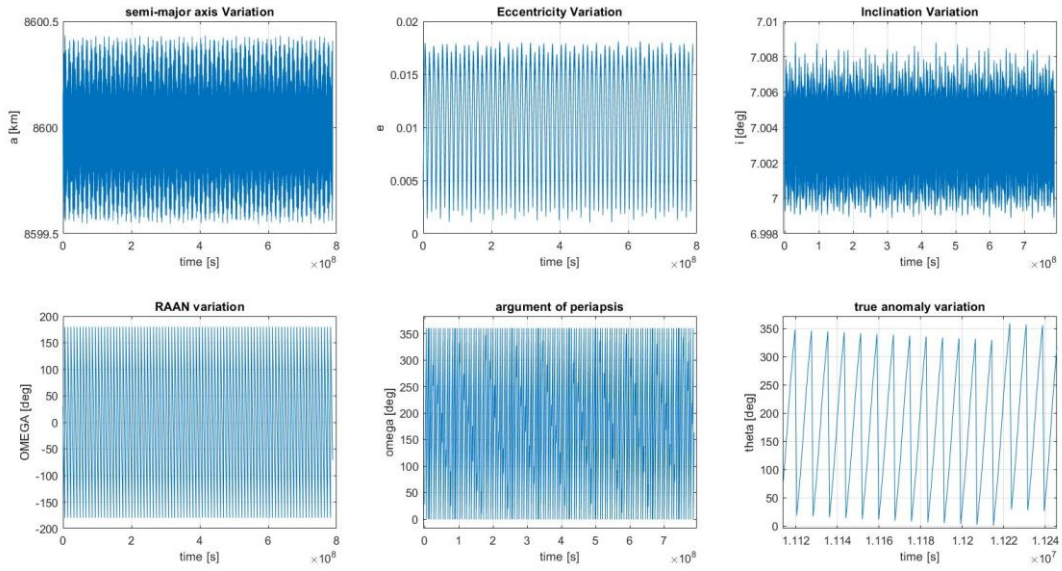

Figure 2.9 Cartesian Variation over a longer period

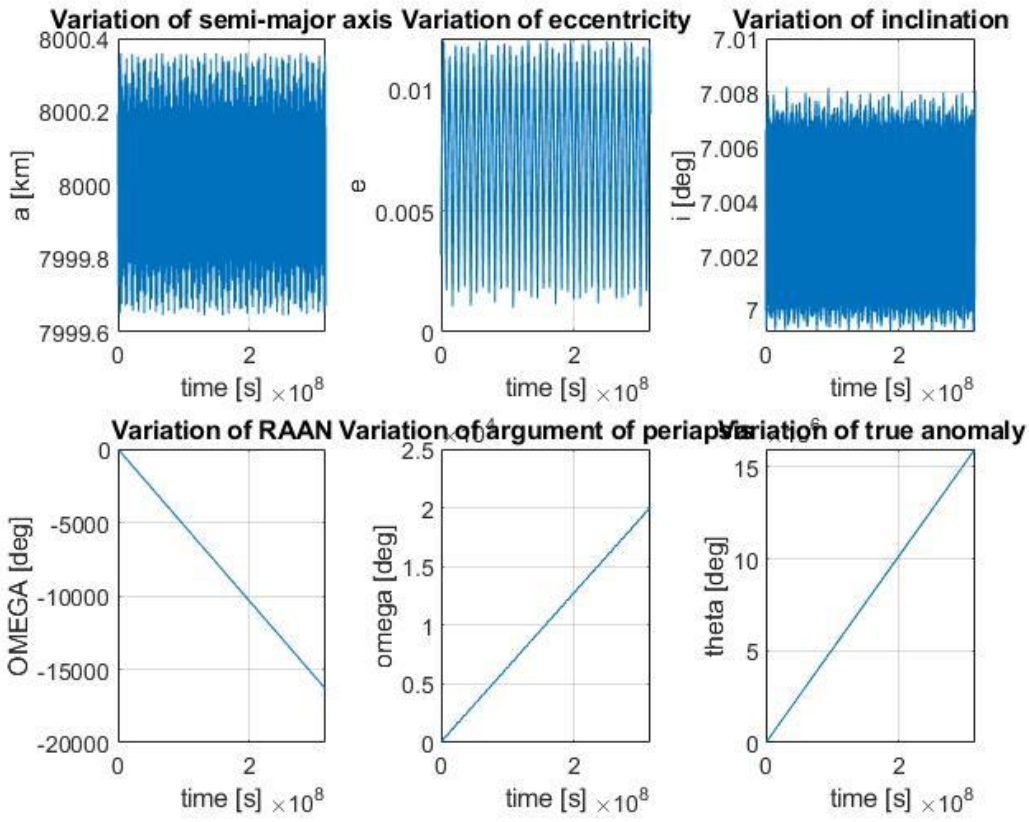

Figure 2.10 Gauss

Hence, from the graphs, it is possible to notice the variations that occur in the orbit propagation.

They can be identified as:

- the *secular variation* of Ω and ω, due to J2 effect
- the *long term oscillation* of *e* and *i*, due to solar radiation perturbation
- the *short term oscillation* of all orbital elements

3.4 Spectral Frequency Analysis

The analysis done before, shows how orbital elements propagate with oscillations, that can be linked to a certain frequency. This allows us to perform a *Spectral Frequency Analysis* in order to obtain a more meaningful representation. Computing the *Fast Fourier Transform (FFT)* of the signal identified by each element's time evolution, we can spot the presence of high frequency harmonics. By the use of a low-pass filter, it is possible to filter the orbital elements propagation, where the long-periodic effects have been associated with 20 orbit revolutions.

At this point we choose to follow this strategy:

> **FFT-based**-filtering
> From the time evolution of the orbital parameters, we apply the *FFT* in order to obtain the frequency spectrum. Then, we use the *low pass filter* to cut off the higher frequencies.

The dominant frequencies for each element are detected using the Fourier analysis based on the oscillating behaviour of the elements. Each signal is expressed in the frequency domain for a better qualitative understanding of the frequency involved. It is achieved by plotting one keplerian parameter at a time.

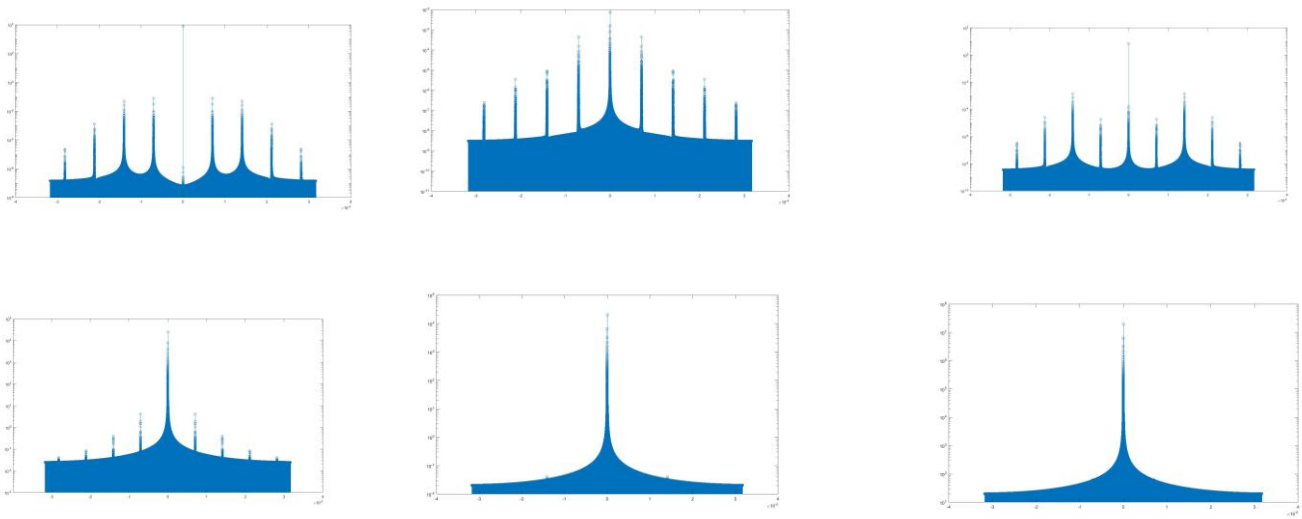

Figure 2.13 Spectra of orbital elements; in order from left to right are: a, e, i, RAAN, omega, theta

The spectral analysis results are here reported above.

The filtering procedure is done using the low-pass filters, where the long-periodic effects have been associated with 20 orbit revolutions. The results are plotted below for long, short periods and secular contributions:

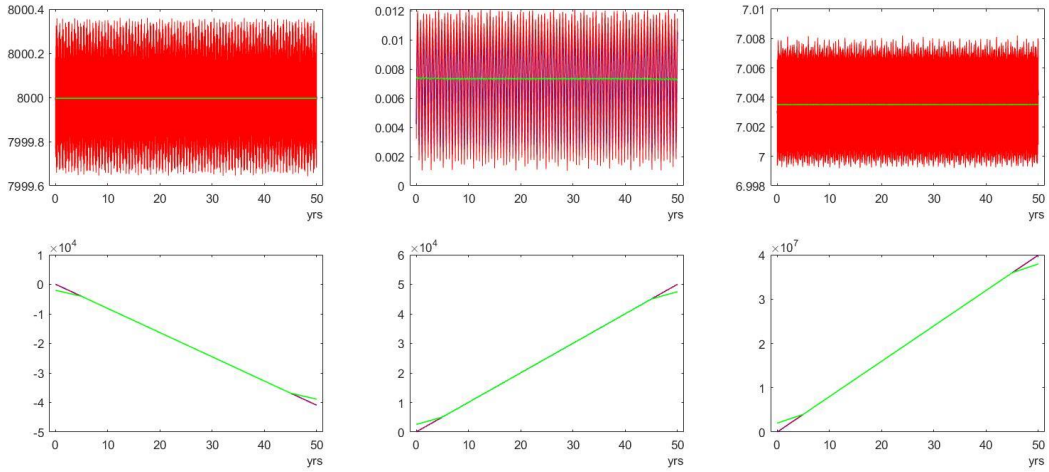

Figure 2.14 Filtering of orbital elements

To have a clearer understanding of variations the graph above has been zoomed for a small window.

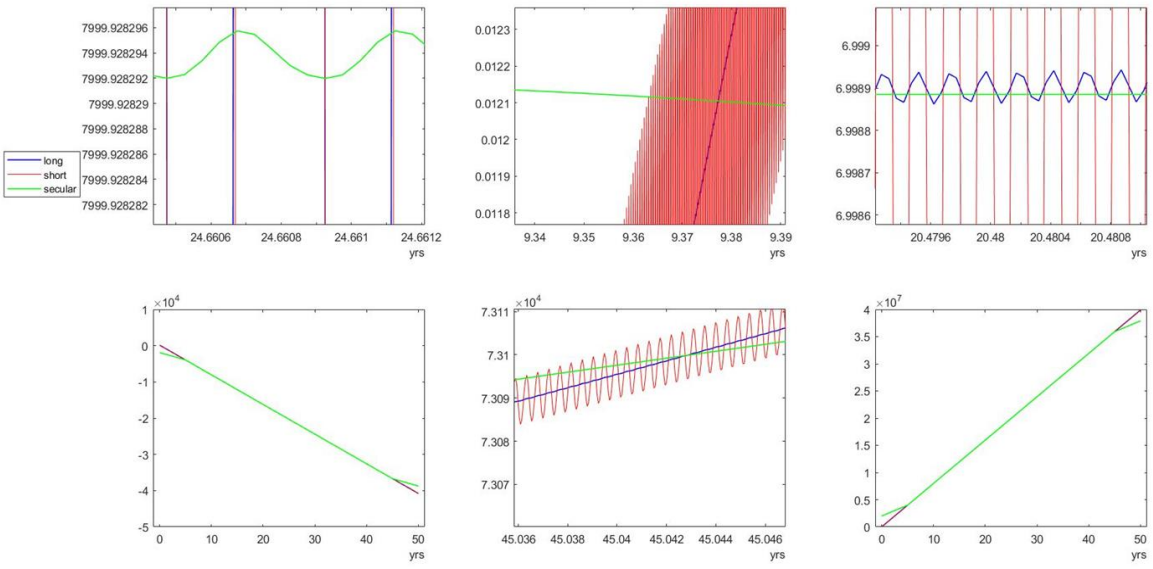

Figure 2.15 Filtering of orbital elements (zoomed)

3.5 Real Data Comparison

In order to compare our data with a real spacecraft data, we chose to show the results produced by the *NASA HORIZONS* for the TDRS-3. The comparison is done considering the trend of keplerian elements over the periods of about 4 months, with our model. This was achieved by finding the ephemeris of the former in NASA JPL HORIZON website. The orbital elements were closer to the data used in the project.

(a= 4000 km, e= 0.003, i= 9°)

The required keplerian elements were extracted and compared with our propagation for 4 months starting from 2015 April 1st. Gauss propagation method, being the relatively efficient one, was used. The results of the comparison are displayed below.

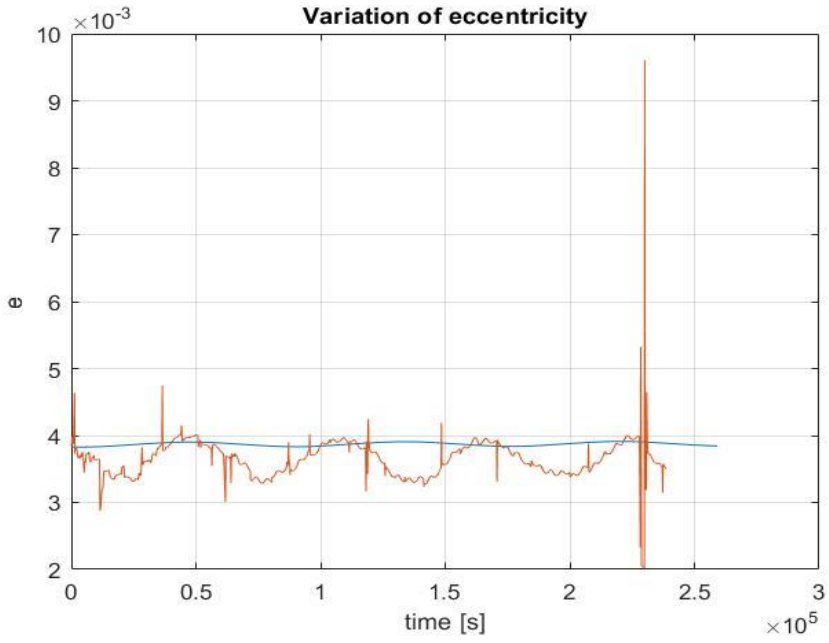

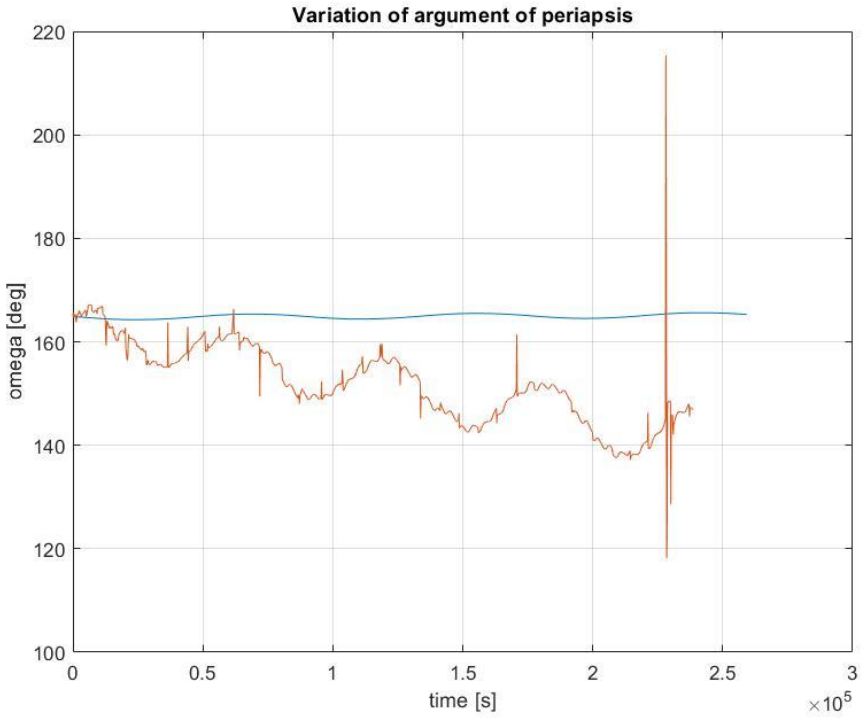

Either way, we saw there is a huge spike in variation along the propagation. This could be because of the other perturbations like the *Moon* and *Drag* that have not been considered.

4. SOURCES

Howard D Curtis. Orbital mechanics for engineering students. Butterworth- Heinemann, 2013.

Nasa HORIZONS. https://ssd.jpl.nasa.gov/horizons.cgi

Richard H Battin. An Introduction to the Mathematics and Methods of Astrodynamics, revised edition. American Institute of Aeronautics and Astronautics, 1999.

David A Vallado. Fundamentals of astrodynamics and applications. Vol. 12. Springer Science & Business Media, 2001.